01 Jan 2024

Ultra-Fast Annealing Improves SNR and Long-term stability of a Highly Multiplexed Line-by-Line FBG Array Inscribed by Femtosecond Laser in a Coreless Fiber for Extreme-Temperature Applications

Farhan Mumtaz
Missouri University of Science and Technology, mfmawan@mst.edu

Bohong Zhang

Jeffrey D. Smith
Missouri University of Science and Technology, jsmith@mst.edu

Ronald J. O'Malley
Missouri University of Science and Technology, omalleyr@mst.edu

et. al. For a complete list of authors, see https://scholarsmine.mst.edu/ele_comeng_facwork/5195

Ultra-Fast Annealing Improves SNR and Long-term stability of a Highly Multiplexed Line-by-Line FBG Array Inscribed by Femtosecond Laser in a Coreless Fiber for Extreme-Temperature Applications

Farhan Mumtaz, *Member IEEE,* Bohong Zhang, *Member IEEE*, Jeffrey D. Smith, Ronald J. O'Malley, Rex Gerald II, and Jie Huang, *Senior Member, IEEE*

***Abstract*—This study reports the fabrication of an 4th-order line-by-line Fiber Bragg Gratings (FBG) array using femtosecond laser inscription within a highly multimode coreless optical fiber, with a particular focus on achieving substantial multiplexing capabilities. An ultra-fast annealing procedure is employed, resulting in an impressive enhancement of the FBG sensor's fringe visibility by approximately 13 dB, signifying a notable improvement of approximately ~4 dB. This substantial enhancement contributes to the long-term stability and performance of the multiplexed FBG array in extreme temperature conditions. The systematic fabrication approach employed for the multiplexed FBG array guarantees a high signal-to-noise ratio (SNR) for each individual FBG within the array. This FBG array is intended for extreme temperature applications, addressing limitations associated with traditional FBGs based on doped optical fibers, including SNR degradation and temperature-induced fringe drift. Testing at temperatures up to 1120°C demonstrates the FBG array's stability without fluctuations in readings. Furthermore, it endures seven heat cycles, spanning from 500°C to 1120°C, over 60 hours, exhibiting outstanding thermal stability. This highly multiplexed FBG array with an ultra-fast annealing approach holds promise for extreme temperature environments, such as steelmaking, where precise and reliable distributed temperature monitoring is imperative.**

***Index Terms*— Ultra fast annealing; coreless Fiber Bragg Grating; line-by-line method; femto-second laser fabrication; highly multimode waveguide.**

I. INTRODUCTION

FIBER gratings play a crucial role as in-fiber optical filters and reflectors in telecommunication systems, fiber lasers, and sensor applications [1], [2]. Traditional FBG, fabricating a wavelength mirror or filter, is created by exposing optical fiber to ultraviolet (UV) laser light [3], thereby inducing periodic refractive index modulation via interferometry or the phase mask technique [4]. However, this conventional method leads to type-I refractive index modulation in optical fibers, limiting the operating temperatures to below 450°C. The demand for sensing capabilities in challenging environments, such as those encountered in the oil and gas industries, power stations, aircraft engines, and furnaces, necessitates the ability to operate FBG sensors at elevated temperatures ranging from 400°C to 1,800°C [5]. Furthermore, conventional FBGs inscribed within telecommunication single-mode fibers (SMFs) often lack sensitivity to vector bending and are therefore unsuitable for numerous applications, including medical instruments. To address the limitations posed by UV lasers [6], researchers have introduced femtosecond laser written FBGs [7], [8]. Effective refractive index modulation can be achieved in a wide range of optical materials, even in non-photosensitive optical fibers, by utilizing femtosecond laser pulses [9]. Presently, three key fabrication technologies have been developed for the production of FBGs in various optical fiber types. These technologies encompass femtosecond laser phase mask technology, femtosecond laser holographic interferometry, and femtosecond laser direct writing technology [10].

Martinez et al. [11] reported the inscription of FBGs using a near-infrared femtosecond laser point-by-point (PbP) technology. Subsequently, they successfully inscribed FBGs through the fiber coating using this technology [12], resulting in FBGs with excellent mechanical strength. However, it should be noted that the refractive index modulation induced by the femtosecond laser PbP technology is not uniform across the fiber's cross-section, leading to a transmission spectrum of the FBG that exhibits strong coupling to cladding modes [13]. To address this issue, it was demonstrated that the fabrication of FBGs in thin core fibers, effectively reduced the coupling to cladding modes [14]. Moreover, the non-uniform modulation cross-section can introduce grating birefringence, resulting in a high polarization-dependent loss of the FBG [15]. Most research reports focused on Single-Mode Fiber (SMF) - based

This paragraph of the first footnote will contain the date on which you submitted your paper for review.

This material is based upon work supported by the U.S. Department of Energy's Office of Energy Efficiency and Renewable Energy (EERE) under the Advanced Manufacturing Office (AMO) Award Number DE-EE0009119. The views expressed herein do not necessarily represent the views of the U.S. Department of Energy or the United States Government.

Corresponding authors:
(Farhan Mumtaz, mfmawan@mst.edu ; Jie Huang, jieh@mst.edu,).

Farhan Mumtaz, Bohong Zhang, Rex Gerald II and Jie Huang are with the Department of Electrical and Computer Engineering, Missouri University of Science and Technology, Rolla, MO 65409 USA.

Jeffrey D. Smith and Ronald J. O'Malley is with the Department of Material Science and Engineering, Missouri University of Science and Technology, Rolla, MO 65409 USA.

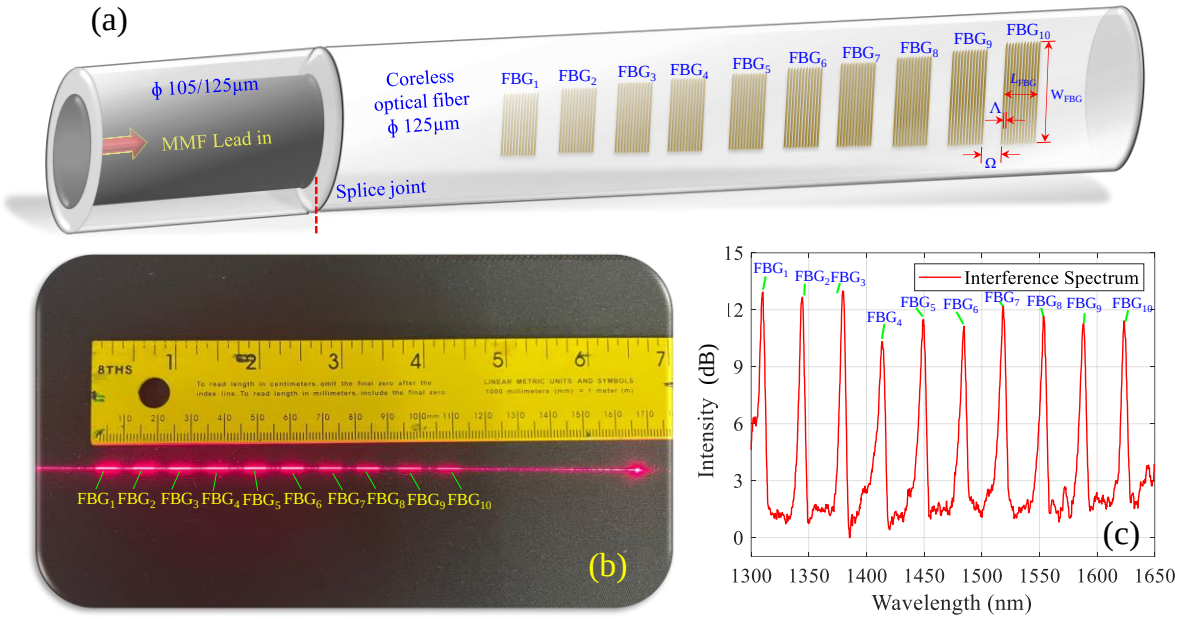

Fig. 1 (a) Schematic representation of a highly multiplexed multimode coreless FBG array, (b) illumination of red laser depicts the positions of fabricated FBGs from FBG_1 to FBG_{10}, and (c) interferogram displays the FBG peak corresponding to each FBG.

FBGs. It was demonstrated that FBGs fabricated in conventional SMFs are unable to withstand temperatures exceeding 1000°C, as the fiber tends to become excessively brittle at such elevated temperatures [16]. To address this issue and enable the FBG's fabrication designed for high-temperature operation, one promising approach involves the utilization of undoped optical fibers, such as Pure Fused Silica Photonic Crystal Fibers (PCFs) [17], [18] and coreless fibers [19], [20]. These fibers offer the advantage of avoiding dopant diffusion at high temperatures but are relatively expensive product.

Few investigations have delved into the creation of FBGs within all-silica PCFs or coreless fibers, primarily for applications requiring high-temperature resistance. For instance, Fu et al. [21] were pioneers in the field, reporting the fabrication of FBGs in PCFs using a UV femtosecond laser. However, their findings revealed that these FBGs began to degrade at a temperature of 500°C. The presence of air hole layers within the PCF cladding induced strong scattering and distortion of the incident femtosecond laser beam, impeding the formation of a type II grating. To address this challenge, Warren-Smith et al. [22] successfully fabricated type II FBGs in pure-silica suspended-core PCFs, which exhibited stability at temperatures up to 1300°C. Furthermore, researchers at Shenzhen University developed an inscription method for PCFs employing a phase mask and an infrared femtosecond laser. By selectively inflating a segment of a commercial PCF, it could be transformed into a suspended-core fiber (SCF) with a simplified cladding structure, enabling lateral access to the core region with minimal loss [23]. The FBG fabricated within the SCF demonstrated exceptional transmission and reflection spectra, coupled with enhanced thermal stability. Even at elevated temperatures, the fabricated FBG within the SCF remained stable, enduring 1000°C for 10 hours before exhibiting any signs of degradation. More recently, our research group introduced an innovative design for large-scale cascade FBG sensors based on pure silica coreless fiber using PbP method [20]. These sensors demonstrated remarkable thermal stability, withstanding temperatures of up to 1100°C for a continuous 24-hour period.

Laser radiation, depending on its intensity, can lead to two distinct refractive index regimes. When the fiber is exposed to relatively low light intensity, it results in a reversible RI modification in the core, which can be partially or fully eliminated at relatively low temperatures [24]. This change in the refractive index can be completely removed by annealing at temperatures below 700 °C, leading to what are known as "type I gratings." On the other hand, when the illumination intensity is relatively high, surpassing the self-focusing threshold, it induces a permanent alteration in the refractive index through multiphoton and avalanche ionization, leading to plasma formation. These are referred to as "type II gratings," and they can endure temperatures higher than 700 °C without experiencing any degradation. Even though pre-annealing can enhance stability, the reliance on factors such as dopants, composition, and exposure conditions makes extremely challenging to establish a one-size-fits-all pre-annealing procedure [25].

Various techniques have been developed thus far to enhance the heat resistance of FBGs. These methods include customizing the glass composition [26], [27], implementing specific thermal cycling or annealing procedures on the gratings [25], [28] and creating gratings through the use of femtosecond lasers [29]–[31]. While researchers have achieved temperature measurements up to 1100 °C, they are still in pursuit of novel approaches that simplify the manufacturing process and reduce costs. One promising solution in this regard is Regenerated Fiber Bragg Gratings (R-FBGs) [32]–[34], which capitalize on a straightforward thermal annealing process but are quite

lengthy. R-FBGs have effectively demonstrated their ability to withstand operating temperatures of up to 1100 °C. During thermal regeneration, a seed grating gradually diminishes as the annealing temperature ascends toward the "regeneration point." Further annealing at elevated temperatures leads to the regrowth of the grating. The regeneration process can be facilitated by either using high germania-content fiber and hydrogen loading before the initial grating inscription [35] or employing helium-loaded germanosilicate optical fiber [36].

Poumellec [37] reported correlation between stability and the inscription of Bragg gratings in disordered materials, particularly focusing on materials like silica, which aligns with the focus of our research. The research introduces a theoretical framework grounded in a reversible physico-chemical equation, which depends on a disorder activation energy. This phenomenon can be attributed to the generation of more stable sites at higher temperatures, where more intricate pathways are employed. Conversely, stability experiences an enhancement during annealing treatment, as it reinitiates more straightforward pathways, consequently eliminating less stable sites. It's worth noting that these conclusions aren't contingent on the specific distribution function, but rather hinge on the assumption of a common saddle point between the processes of writing and erasure.

Drawing inspiration from the ultra-fast sintering method [38] employed in ceramic material synthesis with resistive carbon heater, we have devised an innovative approach for the ultra-fast heat treatment of coreless FBG array. This approach entails the use of a graphite heater for pre-annealing, which promotes stress relief of FBGs within the coreless fiber and holds stability at elevated temperatures. This stress relief is governed by the demarcation energy during fs-laser fabrications, and all defects possessing activation energies below this demarcation energy value are presumed to be eliminated with heat treatments [25]. Consequently, the resulting FBG undergoes what we refer to as "isochronal annealing," characterized as ultra-fast heat treatment in this study. Extending our previous research endeavors [20], [39], this study delves deeper into the possibilities of ultra-fast heat treatment for the annealing of FBGs within an array. The investigation also encompasses the development of a multi-point distributed sensing network tailored to function effectively under extreme temperature conditions, where conventional doped optical fibers have proven to be insufficient. To address this challenge, we have developed a 4^{th}-order line-by-line FBG array with high fringe visibility via an ultra-fast annealing approach. The FBG array incorporates 10 FBGs arranged in a series and facilitates the monitoring of distributed temperature up to 1120°C and encompasses diverse heat treatments spanning a duration of 60 hours across seven heat cycles, with temperature ranges varying from 500°C to 1120°C. The primary objective is to illustrate the exceptional thermal stability of the FBG array, catering to the demands of high-temperature applications, such as steel manufacturing, oil and gas, power generation facilities, aircraft engines, and industrial furnaces. Notably, this study reports for the first time, to the best of our knowledge, of a highly multiplexed FBG array that has undergone ultra-fast heat treatment for annealing, resulting in a substantial improvement in SNR, demonstrating excellent stability under extreme temperature conditions.

TABLE I
FABRICATION PARAMETERS FOR THE PROPOSED MULTIPLEXED FBGS

FBG#	n_{eff}	Λ (μm)	λ_{Bragg} (nm)	No. of reflectors	L_{FBG} (mm)	W_{FBG} (μm)
FBG_1	1.45050	1.806	1309.86	3,378	6.1	42
FBG_2	1.45028	1.854	1344.21	3,344	6.2	44
FBG_3	1.44999	1.903	1379.75	3,311	6.3	46
FBG_4	1.44964	1.951	1413.84	3,280	6.4	48
FBG_5	1.44928	2.000	1449.34	3,250	6.5	50
FBG_6	1.44892	2.049	1484.77	3,222	6.6	52
FBG_7	1.44861	2.097	1518.38	3,195	6.7	54
FBG_8	1.44836	2.146	1554.69	3,169	6.8	56
FBG_9	1.44822	2.194	1588.16	3,144	6.9	58
FBG_{10}	1.44820	2.243	1624.58	3,121	7	60

II. FABRICATION AND SENSOR DESIGN

The inscription of multiplexed FBG array within a coreless multimode optical fiber was accomplished using a femtosecond laser system, specifically the Spirit One model manufactured by Spectra-Physics. This laser system delivered pulses with durations of less than 400 fs and operated at a repetition rate of 200 kHz. To enable the fabrication of coreless FBGs, the laser system was seamlessly integrated with a highly efficient second harmonic generation module, affording the versatility to switch the laser's central wavelength within the range of 520 nm to 1040 nm. Customization of the laser allowed it to operate at 520 nm with a repetition rate of 5 kHz and pulse energy of 500 nJ. Precise control over 3-dimensional displacement was achieved through a translation stage assembly (Newport, XMS100) incorporated into the workstation, delivering an accuracy of 0.05 μm along the x-axis and providing a resolution of <1 nm along the y and z-axes. Laser power management was effectively accomplished using a combination of a half-wave plate and a Glan-laser polarizer seamlessly integrated into the femtosecond laser workstation. The fs laser pulses were directed through a dichroic mirror and focused into the optical fiber via a 40X non-immersion objective lens. Real-time monitoring of fiber alignment and the FBG inscription process was facilitated with the aid of a CMOS camera. The entire microfabrication system was under the precise control of a computer through a graphical user interface (GUI). The fabrication of FBG reflectors, utilizing a line-by-line approach, necessitated the use of an optimized pulse repetition rate and high laser intensity. These parameters were carefully selected to yield an ideal spot size and an equivalent grating period consistent with theoretical calculations, as elaborated in Table I. The order of the FBG is characterized by the equation,

$$m\lambda_{\text{Bragg}} = 2n_{eff}\Lambda \quad (1)$$

where, "m = 4" corresponding to the order of the proposed FBG array. The parameter "n_{eff}" represents the effective refractive index of the fiber, and Λ denotes the grating period. However, a detailed discussion of multimode line-by-line FBG theory, in connection with couple mode theory, has been presented in our earlier study [40]. The schematic representation of the proposed multiplexed FBG array within a coreless fiber is depicted in Fig. 1(a), while the camera image of the fabricated array is presented in Fig. 1(b), and the resulting interferogram is illustrated in Fig. 1(c). The length of each FBG in the array, denoted as L_{FBG}, was adjusted individually across the range of 6.1 mm to 7 mm for FBG_1 through FBG_{10}. Simultaneously, the width of the reflectors, represented as W_{FBG}, was adjusted within the range of 42 µm to 60 µm. This fine-tuning of the reflector width was performed to ensure the maintenance of an optimal extinction ratio for each FBG in the resulting interferogram. It's important to note that the spacing between adjacent FBGs, represented as Ω, was kept constant at 5 mm for each FBG, which can be increased or decreased according to need of different applications, for example tundish lining, refractory line, furnaces in steel making industry. Throughout the fabrication process, the intensity of the acousto-optic modulator (AOM) was consistently maintained at 10%, and the laser scanning velocity was set at a constant rate of 80 µm/s for all FBGs within proposed configuration. The line-by-line pattern of an FBG inscribed in the coreless fiber, highlighting both a top-view and a lateral view, is displayed in Fig. 2(a-b), respectively. For visualizing the cross-sectional view of the utilized fibers (coreless and multimode), images were captured under a microscope (specifically, the built-in GPX-3400 microscope from Thorlabs), and these images are showcased in Fig. 2(c-d). Multimode fiber-based FBGs offer several advantages over their single-mode counterparts such as heightened sensitivity to temperature and strain. These benefits arise from their larger mode field diameter and increased overlap between the modes and the grating. Furthermore, they can serve as distributed sensors for measuring temperature or strain along the length of the fiber. However, it's important to note that modal interference and dispersion can introduce complexity into the analysis and impose limitations on FBG performance.

III. Experimental Results and Discussions

Annealing is a pivotal factor affecting the performance of coreless fiber based FBGs, particularly when these FBGs are intended for operation in extreme temperature environments, such as 1100°C. Our previous research demonstrated the effectiveness of slow isothermal annealing in achieving residual stress release and long-term stability [20]. However, this approach, while advantageous, is time intensive. Ultra-fast heat treatment involves rapidly increasing the temperature of a material to a predefined level and maintaining it for a short duration, followed by rapid cooling. The key characteristic of ultra-fast heat treatment is the swift transition between high and low temperatures. This process aims to induce specific changes

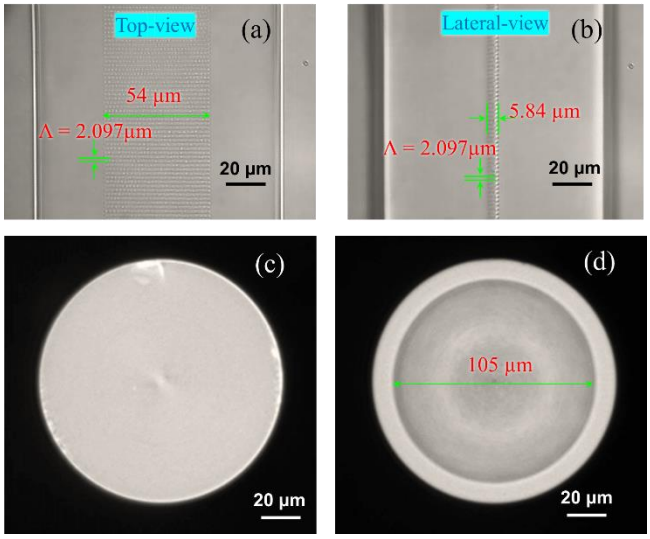

Fig. 2 provides microscopic images illustrating the line-by-line pattern of the FBG inscribed within the coreless fiber, offering both a (a) top-view and (b) lateral view. Additionally, the images display cleaved faced of (c) coreless fiber utilized for sensors and the (d) multimode fiber (MMF) with a core and cladding diameter measuring 105/125 µm for lead-in.

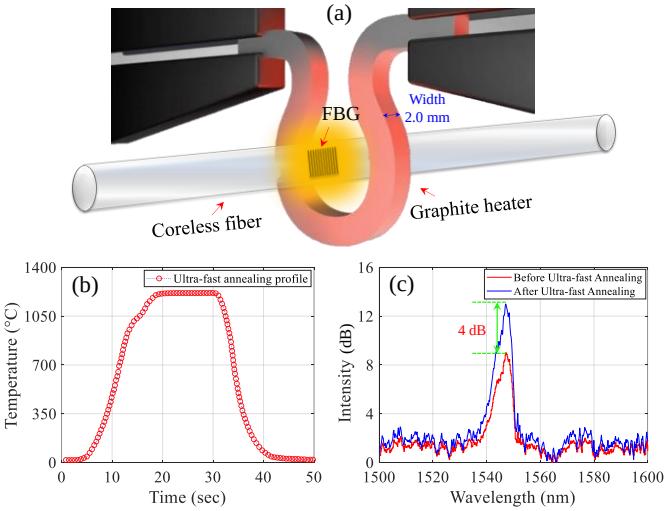

Fig. 3 showcases the ultra-fast heating setup: (a) A schematic representation of the Graphite heater, demonstrating the heating of the FBG; (b) The temperature profile of the heater during ultra-fast heating, reaching up to 1200°C; and (c) Spectra comparison before and after the fast-heating cycles.

in the material's structure, such as stress relief, crystallization, or other thermal modifications, in a much shorter time compared to conventional heat treatment methods. In the context of FBG fabrication, ultra-fast heat treatment can help enhance the performance and stability of the gratings within a significantly reduced timeframe. Isochronal annealing is a heat treatment process where a material is subjected to a series of annealing steps, each at a constant temperature for a specific duration. The term "isochronal" refers to the consistent duration of each annealing step. This method allows researchers to study the evolution of material properties systematically as the

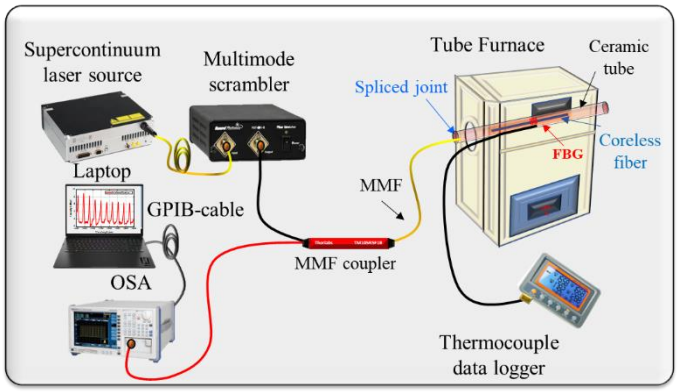

Fig. 4 Experimental setup for calibration of the proposed FBG sensor and data acquisition.

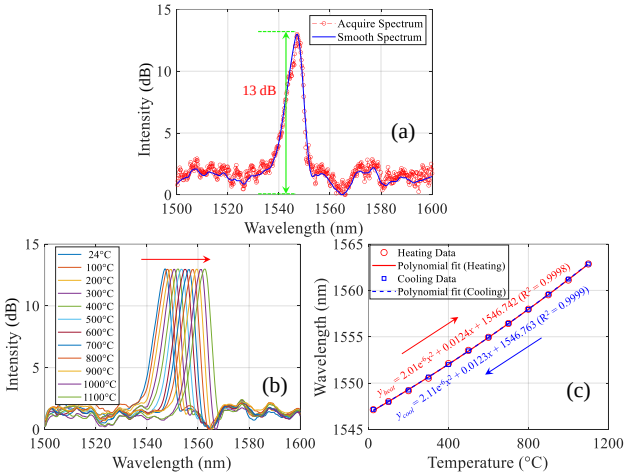

Fig. 5 illustrates key aspects of the single FBG spectra: (a) a comparison between the acquired spectrum and a smoothed spectrum using Savitzky-Golay smoothing, (b) the spectral shift observed during the heat treatment from room temperature to 1100°C, and (c) the curve fitting correlation function depicting the heating and cooling phases of the proposed FBG.

temperature is incrementally changed. In the context of FBGs, isochronal annealing can be employed to tailor the thermal and structural characteristics of the gratings, optimizing their performance for specific applications. By carefully controlling the annealing temperature and duration, researchers can achieve desired modifications in the FBG's refractive index profile and other crucial parameters. In contrast, this study introduces an ultra-fast annealing technique employing a graphite heater integrated with argon gas flow (GPX-3400, Thorlabs). This advanced heating system can reach temperatures of up to 2500°C. In the ultra-fast annealing process for the proposed FBGs, various heating profiles were explored to attain the desired temperature profile. Controlled filament power, managed through a graphical user interface (GUI), resulted in stable temperatures (i.e., 1200°C, 1600°C, and 1800°C corresponding to filament powers of 55W, 75W, and 90W, respectively). Figure. 3(a) illustrates the schematic of the ultra-fast heating setup, the graphite heater employed in the study features a ~2.0 mm width and is equipped with real-time control capabilities, allowing dynamic movement back and forth to maintain a constant temperature, particularly during the set heating time of 10 seconds. This real-time adjustment is crucial for achieving precise temperature control, ensuring that the FBGs undergo the desired annealing process with accuracy and efficiency. In the context of the heating profile, as illustrated in Fig. 3(b), the ramping-up phase, temperature stabilization, and ramping-down phase are clearly delineated. During the ramping-up phase, the temperature gradually increases to the targeted set temperature. Then, graphite heater stabilizes a temperature of 1200°C for the specified duration of 10 seconds. The ramping-down phase follows, gradually decreasing the temperature to complete the annealing process.

Figure. 3(c) showcases the FBG interference spectra before and after ultra-fast heat treatment. The heating cycle, as depicted in Fig. 3(b), was repeated four times. After the initial three cycles, the FBG exhibited a significant increase in maximum fringe visibility, reaching approximately 13 dB. The fourth cycle was executed, but no further improvement in SNR was observed. This observation confirmed that after three cycles, the FBG had achieved its maximum SNR, signifying the complete alleviation of stress within the coreless fiber introduced during fabrication, as supported by the improved FBG SNR. Annealing at elevated temperatures not only facilitates stress relief, allowing the fiber to relax but also encourages structural rearrangements, leading to a more uniform refractive index profile.

Before assessing the performance of the multiplexed FBGs, calibration was conducted on an FBG with a Bragg wavelength of 1546.7 nm. The schematic representation of the experimental setup for calibrating the proposed FBG is presented in Fig. 4. This setup comprises a supercontinuum laser source (SC-5,Wuhan Yangtze Soton Laser) offering a wavelength range of 400-2200 nm, an electronic multimode scrambler (MM-201), an Optical Spectrum Analyzer (OSA) connected with a laptop via a GPIB cable, and a 3 dB multimode coupler (Thorlabs, model #TM105R5F1B) designed for acquiring the reflection spectra of the FBG. The lead-in multimode fiber utilized in this setup had a core diameter of 105 µm and a cladding diameter of 125 µm. To alleviate multimode interferences within the highly multimode coreless fiber, the MM-201 was employed to scramble all the modes carried by the multimode fiber. The calibration process involved utilizing a custom-designed high-temperature furnace (Thermo Scientific® TF55030A-1 Lindberg/Blue M) with a precision of ±1 °C and a maximum temperature capability of 1100°C. A K-type thermocouple, accompanied by a data logger, was employed to record temperature readings. Within the furnace, the FBG was carefully positioned, taking advantage of the controlled furnace heating rate of 10°C per minute. The calibration procedure initiated with the temperature gradually increasing from ambient room temperature to 1100 °C, progressing in 100 °C increments. Conversely, during the cooling phase, the FBG underwent a reverse process, with temperature data being recorded in 100 °C decrements. Throughout both the heating and cooling phases, the temperature remained stable for 30 minutes at each heating

step, while the spectrum was continuously monitored using an OSA. The spectrum of the single FBG is visually depicted in Fig. 5(a), with the application of Savitzky-Golay smoothing to process the spectral shifts during heat treatment at different instances. The spectral evolution of the FBG during the heating process is elaborated in Fig. 5(b). An excellent fit to a 2nd-order polynomial curve was achieved for both heating and cooling phases, exhibiting R-squared values of approximately 0.999, as demonstrated in Fig. 5(c).

The Bragg wavelength shift ($\Delta\lambda_{Bragg}$) for an FBG within a coreless multimode fiber can be estimated as [41],

$$\Delta\lambda_{\text{Bragg}} = \lambda_{\text{Bragg}} - \lambda_{\text{Bragg0}} \quad (2)$$

where, λ_{Bragg} represents the Bragg wavelength at the measured temperature (T), and λ_{Bragg0} is the Bragg wavelength at the reference temperature (T_0). The temperature sensitivity (S_T) of an FBG in coreless multimode fiber can be determined using as [42],

$$S_T = \frac{\Delta\lambda_{\text{Bragg}}}{\Delta T} \quad (3)$$

where S_T represents the temperature sensitivity, and ΔT is the change in temperature that corresponds to $\Delta\lambda_{Bragg}$. However, it's essential to consider that the effective refractive index of an air-clad fiber is typically lower than that of a silica-clad fiber, and this can influence the temperature sensitivity. Additionally, the modal distribution of light in an air-clad fiber differs from that in a silica-clad fiber, which can further impact the FBG's performance. Therefore, it is crucial to account for the specific properties of the fiber when calculating the Bragg wavelength shift and temperature sensitivity. At a certain Bragg wavelength, the temperature change can be estimated as [43],

$$\frac{\Delta\lambda_{\text{Bragg}}}{\lambda_{\text{Bragg}}} = (\alpha + \varepsilon)\Delta T + (1 + \sigma)\varepsilon \quad (3)$$

where $\Delta\lambda_{Bragg}/\lambda_{Bragg}$ represents the relative change in the Bragg wavelength, α stands for the thermal expansion coefficient of the fiber, ε denotes the strain applied to the fiber, and σ represents the photo-elastic constant of the fiber. Given the specific conditions where the fiber was loosely placed into the tube furnace, resulting in ε = 0, the temperature sensitivity of the FBG at λ_{Bragg}= 1546.7 nm can be calculated using eq. (3) and is approximately ~14.7 pm/°C, as indicated in Fig. 5(c). Similarly, the temperature sensitivity for all the FBGs listed in Table I can be determined by correlating the spectral shift observed in their respective spectra during heating or cooling.

The performance and stability assessment of the multiplexed FBG array were conducted under an elevated temperature of 1120°C. To evaluate the distributed temperature performance of the proposed multiplexed FBGs, the sensors were positioned within a furnace designed to create a thermal gradient. These FBGs were mounted vertically using an alumina ceramic two-bore tube within the furnace. Throughout 60-hour duration in extreme environmental conditions, the sensors displayed

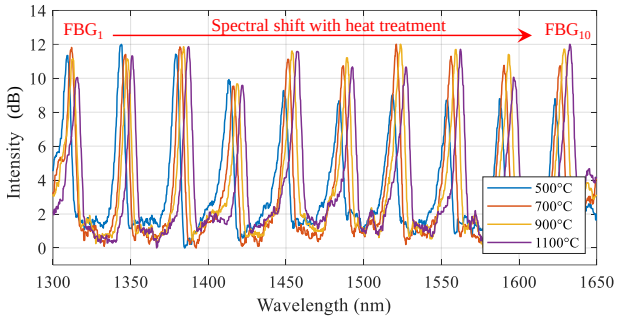

Fig. 6 presents the spectral shift observed in the multiplexed FBGs as the temperature varies from 500°C to 1100°C during stability testing.

exceptional stability. The stability of the multiplexed sensor was systematically monitored through heating and cooling cycles spanning from 500°C to 1120°C. The spectral shifts observed during the heat treatment, ranging from 500°C to 1100°C, are depicted in Fig. 6. It is notable that the fringe visibility of the FBG peaks exhibits a clear improvement as the temperature increases. Throughout the stability test, an average peak visibility of ~9 dB was consistently observed. The sensor underwent seven cycles in total, with the FBG sensors exposed to extreme temperatures (i.e., 1120°C) for 30 hours, as depicted in Fig. 7. During the plateau phase, FBG_1 to FBG_{10} exhibited temperature gradients of 1025°C, 1065°C, 1076°C, 1084°C, 1119°C, 1121°C, 1123°C, 1096°C, 1093°C, and 1069°C, with no observable thermal drifting of any FBG. It's worth noting that FBG_5 was positioned in close proximity to a thermocouple, aligning with the obtained temperature profile. Additionally, a 3D and 2D contour temperature profile of the employed furnace was generated using MATLAB code, providing a distributed temperature mapping of the multiplexed FBG sensors. It was observed that the maximum temperature was recorded by FBG_5 to FBG_7 sensors, indicating a region of uniform temperature within the furnace. In contrast, the remaining FBG sensors exhibited slightly lower readings, as illustrated in Fig. 8(a-b). This underscores the potential advantages of the proposed multiplexed configuration of FBG sensors for recording temperature profiles, thermal gradients, and pinpointing hotspot regions with reliability.

For the proposed sensing structure, the absence of a bounded cladding layer in the coreless multimode fiber eliminates potential issues such as dopant migration associated with low-index contrast cladding. Traditional multimode fibers with low-index contrast cladding materials can experience stress-related problems at high temperatures, up to 1100°C, including dopant migrations [44] and Bragg wavelength drift [45]. However, in the case of a coreless structure with an air cladding, the risk of stress- induced effects or Bragg wavelength drifting at elevated temperatures is entirely mitigated. The elimination of stress arising from thermal expansion mismatch between the core and cladding materials in the coreless fiber significantly reduces stress, enhancing the stability of its optical characteristics through fast heat annealing. This leads to improve signal propagation and minimizes signal degradation. The absence of stress-induced effects, such as dopant migrations and

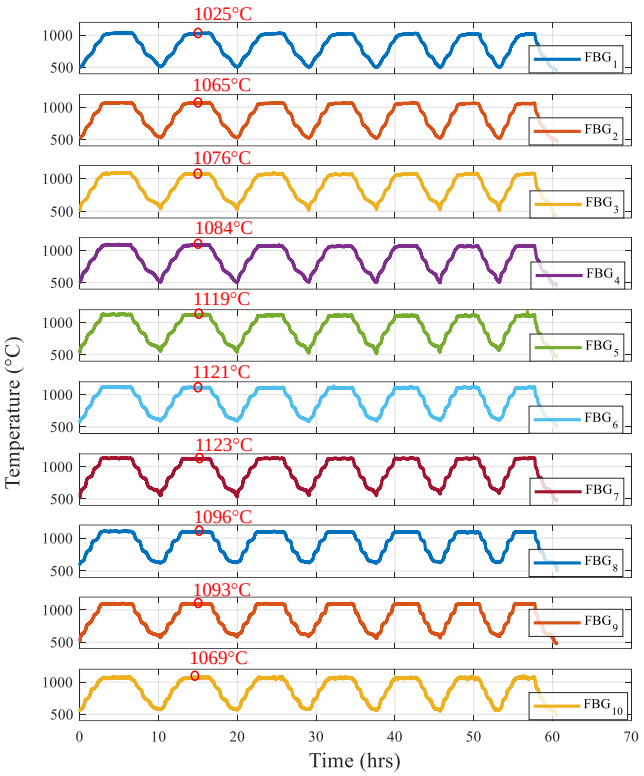

Fig. 7 showcases the stability performance of the multiplexed FBG sensors as they undergo seven cycles of heating and cooling phases during 60 hours of exposure to extreme temperature conditions.

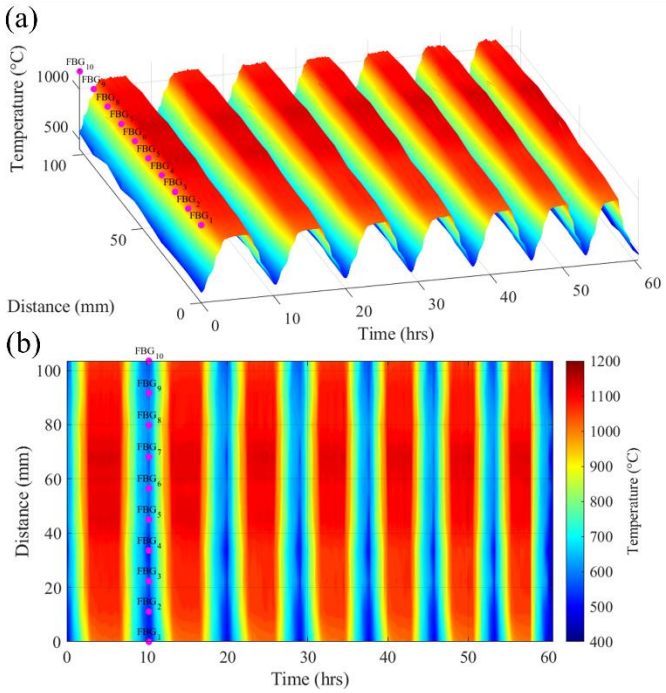

Fig. 8 illustrates the contour profile depicting the heating and cooling cycles of temperature data inside the employed furnace, captured by a multiplexed array of FBG sensors, designated as FBG_1 to FBG_{10}. The visualization is presented in two formats: (a) a three-dimensional (3D) profile and (b) a two-dimensional (2D) profile, corresponding to the spatial locations of each FBG sensor within the multiplexed configuration.

wavelength drift, guarantees that the coreless fiber maintains its optical performance and integrity, even when exposed to high-temperature conditions. This innovative ultra-fast annealing approach holds promise for enhancing the stability and performance of coreless fiber-based FBGs in extreme temperature environments.

The stability of peak intensity in the proposed multiplexed FBG array at elevated temperatures was also investigated. Over a 60-hour period, a close monitoring of intriguing peak intensity fluctuations within the multiplexed FBG array during a series of heating cycles was carried out. In Figure 9, a comparison of the multiplexed FBG array's peak intensities at various time intervals ~ 5, 15, 25, 35, 50, and 60 hours is presented, while keeping the furnace temperature stable at 1120°C. The accompanying panels in the study visually illustrate the interference spectra of the multiplexed FBG array at different time points during the 60-hour heating cycles, showing a consistent behavior of the FBGs when the temperature reached its peak of 1120°C. Figure 10 provides a 2D profile that depicts the fluctuations in peak intensity within the multiplexed FBG array across the heating, cooling, and stabilized phases. Notably, the recorded peak intensity fluctuations ranged within ±1 dB, transitioning from cooling to heating phases. However, as the temperature stabilized at its maximum of 1120°C, the FBG peaks exhibited remarkable stability, with fluctuations narrowing to just ±0.5 dB. In multiplexed FBG array, where FBGs are closely spaced and interact with each other, their multimodal interference behavior can lead to complex interactions. The reported intensity fluctuations within ±0.5 dB suggest that the design and configuration of the multiplexed FBG array have been carefully optimized to minimize crosstalk and interference effects between the individual FBGs during different phases of the annealing process. This optimization is crucial for ensuring the reliability and accuracy of the FBG array's performance, especially in applications where precise and stable sensing is required. The controlled intensity fluctuations demonstrate the effectiveness of the design in mitigating the influence of one FBG on another within the multiplexed array, ultimately enhancing the overall performance of the sensing system.

This research also provides the potential limitations and challenges linked to deploying the multiplexed FBG array in diverse industrial sectors. A significant challenge arises from the varying environmental conditions across different industries, potentially impacting the performance and durability of the FBGs. Harsh environments in sectors like oil and gas or aerospace may pose challenges for long-term stability, particularly if the FBG array is exposed beyond temperature limits, such as exceeding 1200°C. Addressing these challenges involves developing protective refractory linings or enclosures for the FBG array to enhance its resilience to environmental factors. Additionally, the need for customized parameter optimization for different industrial applications introduces a

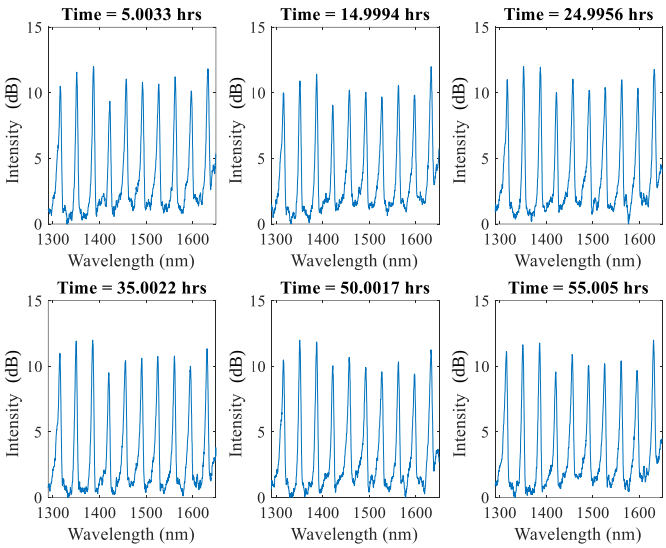

Fig. 9 Panels display the interference spectra of a multiplexed FBG array at various time intervals during 60 hrs of heating cycles when the temperature was stabilized at its maximum temperature of 1120°C.

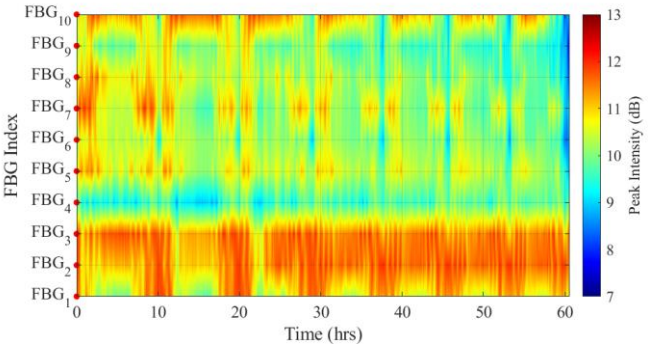

Fig. 10 illustrates the peak intensity fluctuation profile of a multiplexed FBG array during a 60-hour time span while undergoing heating cycles. The recorded peak intensity fluctuations range is ±1 dB (from cooling to heating phases), with FBG peaks exhibiting fluctuations of ±0.5 dB at stabilized temperatures.

potential challenge in terms of scalability. To overcome this, standardized protocols for parameter tuning and deployment could be established, ensuring adaptability across diverse sectors. Moreover, the integration of advanced signal processing techniques, such as the Multimode Bayspec interrogation system, can be explored to mitigate issues related to signal degradation in complex industrial settings. Overall, the research insights provide a foundation for considering these challenges and suggest avenues for further investigation and development to optimize the performance of the multiplexed FBG array in diverse industrial contexts.

The proposed highly multiplexed FBG array emerges as a compelling solution, particularly in scenarios where conventional sensors like single-mode fiber Bragg gratings [4] and Rayleigh optical frequency domain reflectometry (OFDR) [46] fall short due to their limited tolerance for extreme temperatures. In critical applications within the steelmaking industry, such as tundish lining, roller casting, submerge entry nozzle refractory, and heating furnace are exposed to exceedingly high temperatures. The exhaustive 60-hour testing regime, featuring cyclic rounds of heating and cooling, has demonstrated the exceptional durability and stability of these multiplexed FBG array in extreme environments (1120°C). This breakthrough not only positions these sensors as ideal candidates for high-temperature applications in steelmaking but also extends their relevance to diverse industrial sectors including oil and gas, jet engines, turbines, and furnaces. The thermal distributed mapping of these applications are crucial for ensuring the structural health. In these settings, the ability to measure distributed temperature profiles is pivotal for ensuring operational stability, enhancing efficiency, optimizing product yield, and ultimately contributing to substantial energy cost savings. The proposed multiplexed FBG array thus represent a versatile and robust solution with far-reaching implications for industries reliant on precise temperature monitoring in challenging conditions.

V. Conclusion

In conclusion, this research demonstrates a significant leap forward in the arena of high-temperature distributed sensing through the development and characterization of a highly multiplexed FBG array. Leveraging the distinctive characteristics of coreless fiber-based FBGs and employing an ultra-fast annealing approach, these FBGs have exhibited remarkable stability and durability in extreme temperature environments, enduring testing at temperatures as high as 1120°C for extended durations. This achievement signifies a substantial advancement in optical sensing capabilities, particularly when compared to their single-mode counterparts and other established sensing technologies (limited to survivability up to 700°C [4], [46]). The proposed study has provided comprehensive insights into the fabrication process, encompassing fs-laser parameters, FBG array designing, ultra-fasting annealing, and calibration techniques, ensuring the reproducibility and reliability of these sensors for practical applications. The extensive testing and characterization efforts undertaken, coupled with the robustness and steadfastness exhibited by FBG array, position them as pioneering solutions for high-temperature distributed sensing across a spectrum of industrial domains. The proposed multiplexed FBG array versatility extends beyond the steelmaking sector, encompassing applications in oil and gas, jet engines, turbines, and furnaces, among others. The ability to meticulously monitor distributed temperature profiles in such demanding settings holds great promise for enhancing operational stability, improving efficiency, optimizing product yield, and ultimately contributing to substantial energy cost savings.

Acknowledgment

This material is based upon work supported by the U.S. Department of Energy's Office of Energy Efficiency and Renewable Energy (EERE) under the Advanced Manufacturing Office (AMO) Award Number DE-EE0009119. The views

expressed herein do not necessarily represent the views of the U.S. Department of Energy or the United States Government.

REFERENCES

[1] C. Zhu, R. E. Gerald, and J. Huang, "Progress Toward Sapphire Optical Fiber Sensors for High-Temperature Applications," *IEEE Trans Instrum Meas*, vol. 69, no. 11, pp. 8639–8655, 2020, doi: 10.1109/TIM.2020.3024462.

[2] D. R. Viveiros, J. M. Maia, V. A. Amorim, P. A. Jorge, and P. V. Marques, "Fabrication of periodic structures in optical fibers by femtosecond laser micromachining for sensing applications," in *In Fourth International Conference on Applications of Optics and Photonics*, 2019, p. 69. doi: 10.1117/12.2527261.

[3] D.-N. Wang, "Review of femtosecond laser fabricated optical fiber high temperature sensors [Invited]," *Chinese Optics Letters*, vol. 19, no. 9, p. 091204, 2021, doi: 10.3788/col202119.091204.

[4] F. Shang, J. Tang, W. Gan, H. Guo, and M. Yang, "Fast thermal regeneration of weak fiber Bragg gratings," *Optics InfoBase Conference Papers*, vol. 38, no. 20, pp. 4178–4181, 2018, doi: 10.1364/OEDI.2018.OT4A.27.

[5] J. He, B. Xu, X. Xu, C. Liao, and Y. Wang, "Review of Femtosecond-Laser-Inscribed Fiber Bragg Gratings: Fabrication Technologies and Sensing Applications," *Photonic Sensors*, vol. 11, no. 2, pp. 203–226, 2021, doi: 10.1007/s13320-021-0629-2.

[6] S. J. Mihailov *et al.*, "Extreme environment sensing using femtosecond laser-inscribed fiber bragg gratings," *Sensors (Switzerland)*, vol. 17, no. 12, 2017, doi: 10.3390/s17122909.

[7] K. A. Zagorulko *et al.*, "Fabrication of fiber Bragg gratings with 267 nm femtosecond radiation," *Opt Express*, vol. 12, no. 24, p. 5996, 2004, doi: 10.1364/opex.12.005996.

[8] M. Bernier, R. Vallée, B. Morasse, C. Desrosiers, A. Saliminia, and Y. Sheng, "Ytterbium fiber laser based on first-order fiber Bragg gratings written with 400nm femtosecond pulses and a phase-mask," *Opt Express*, vol. 17, no. 21, p. 18887, 2009, doi: 10.1364/oe.17.018887.

[9] R. Chen, J. He, X. Xu, J. Wu, Y. Wang, and Y. Wang, "High-Quality Fiber Bragg Gratings Inscribed by Femtosecond Laser Point-by-Point Technology," *Micromachines (Basel)*, vol. 13, no. 11, 2022, doi: 10.3390/mi13111808.

[10] R. Berlich, D. Richter, M. Richardson, and S. Nolte, "Fabrication of computer-generated holograms using femtosecond laser direct writing," *Opt Lett*, vol. 41, no. 8, p. 1752, 2016, doi: 10.1364/ol.41.001752.

[11] M. A., D. M., K. I., And, and B. I., "Direct writing of fibre Bragg gratings by femtosecond laser," *Electron Lett*, vol. 41, no. 2, pp. 40–41, 2005, doi: 10.1049/el.

[12] A. Martinez, I. Y. Khrushchev, and I. Bennion, "Direct inscription of Bragg gratings in coated fibers by an infrared femtosecond laser," *Opt Lett*, vol. 31, no. 11, p. 1603, 2006, doi: 10.1364/ol.31.001603.

[13] J. U. Thomas *et al.*, "Cladding mode coupling in highly localized fiber Bragg gratings II: complete vectorial analysis," *Opt Express*, vol. 20, no. 19, p. 21434, 2012, doi: 10.1364/oe.20.021434.

[14] X. Liu *et al.*, "Low short-wavelength loss fiber Bragg gratings inscribed in a small-core fiber by femtosecond laser point-by-point technology," *Opt Lett*, vol. 44, no. 21, p. 5121, 2019, doi: 10.1364/ol.44.005121.

[15] C. Caucheteur, T. Guo, and J. Albert, "Polarization-Assisted Fiber Bragg Grating Sensors: Tutorial and Review," *Journal of Lightwave Technology*, vol. 35, no. 16, pp. 3311–3322, 2017, doi: 10.1109/JLT.2016.2585738.

[16] C. R. Liao and D. N. Wang, "Review of femtosecond laser fabricated fiber Bragg gratings for high temperature sensing," *Photonic Sensors*, vol. 3, no. 2, pp. 97–101, 2013, doi: 10.1007/s13320-012-0060-9.

[17] G. D. Peng, *Handbook of Optical Fibers*. 2019. doi: 10.1007/978-981-10-7087-7.

[18] H. Xiang and Y. Jiang, "Fiber Bragg grating inscription in multi-core photonic crystal fiber by femtosecond laser," *Optik (Stuttg)*, vol. 171, no. June, pp. 9–14, 2018, doi: 10.1016/j.ijleo.2018.06.020.

[19] C. Zhu, O. Alsalman, and J. Huang, "Fs-Laser Fabricated Miniature Fabry–Perot Interferometer in a No-Core Fiber for High-Temperature Applications," *Sensors*, vol. 23, no. 18, p. 7754, 2023, doi: 10.3390/s23187754.

[20] F. Mumtaz, B. Zhang, R. J. O'Malley, And, and J. Huang, "Large-scale cascading of first-order FBG array in a highly multimode coreless fiber using femtosecond laser for distributed thermal sensing," *Opt Express*, vol. 31, no. 18, pp. 29639–29653, 2023.

[21] F. L.B. *et al.*, "Femtosecond laser writing Bragg gratings in pure silica photonic crystal fibres," *Electron Lett*, vol. 41, no. 11, pp. 40–41, 2005, doi: 10.1049/el.

[22] S. C. Warren-Smith, L. V. Nguyen, C. Lang, H. Ebendorff-Heidepriem, and T. M. Monro, "Temperature sensing up to 1300°C using suspended-core microstructured optical fibers," *Opt Express*, vol. 24, no. 4, p. 3714, 2016, doi: 10.1364/oe.24.003714.

[23] C. Wang *et al.*, "Bragg gratings inscribed in selectively inflated photonic crystal fibers," *Opt Express*, vol. 25, no. 23, p. 28442, 2017, doi: 10.1364/oe.25.028442.

[24] O. Andreas, "Fiber Bragg Gratings," *Rev. Sci. Instrum.*, vol. 4341, no. June 1997, pp. 4309–4341, 2010, doi: https://doi.org/10.1063/1.1148392 ?

[25] E. G. Turitsyna and S. Webb, "Predicting thermal stability of fibre Bragg gratings–isothermal annealing within isochronal annealing," *Electron Lett*, vol. 43, no. 24, pp. 1341–1342, 2007, doi: 10.1049/el.

[26] Y. Shen *et al.*, "Thermal decay characteristics of strong fiber Bragg gratings showing high-temperature sustainability," *Journal of the Optical Society of America B*, vol. 24, no. 3, p. 430, 2007, doi: 10.1364/josab.24.000430.

[27] O. V. Butov, E. M. Dianov, and K. M. Golant, "Nitrogen-doped silica-core fibres for Bragg grating sensors operating at elevated temperatures," *Meas Sci Technol*, vol. 17, no. 5, pp. 975–979, 2006, doi: 10.1088/0957-0233/17/5/S06.

[28] S. K. Abi Kaed Bey, T. Sun, and K. T. V. Grattan, "Optimization of a long-period grating-based Mach-Zehnder interferometer for temperature measurement," *Opt Commun*, vol. 272, no. 1, pp. 15–21, 2007, doi: 10.1016/j.optcom.2006.11.016.

[29] D. Grobnic, S. J. Mihailov, C. W. Smelser, and H. Ding, "Sapphire fiber bragg grating sensor made using femtosecond laser radiation for ultrahigh temperature applications," *IEEE Photonics Technology Letters*, vol. 16, no. 11, pp. 2505–2507, 2004, doi: 10.1109/LPT.2004.834920.

[30] S. J. Mihailov, D. Grobnic, R. B. Walker, H. Ding, F. Bilodeau, and C. W. Smelser, "Femtosecond laser inscribed high temperature fiber Bragg grating sensors," in *Fiber Optic Sensors and Applications V*, 2007, p. 677009. doi: 10.1117/12.742315.

[31] G. D. Marshall and M. J. Withford, "Annealing Properties of Femtosecond Laser Inscribed Point-by-point Fiber Bragg Gratings," in *Optics InfoBase Conference Papers*, 2007, pp. 30–32.

[32] D. Barrera, V. Finazzi, J. Villatoro, S. Sales, and V. Pruneri, "Packaged optical sensors based on regenerated fiber bragg gratings for high temperature applications," *IEEE Sens J*, vol. 12, no. 1, pp. 107–112, 2012, doi: 10.1109/JSEN.2011.2122254.

[33] E. Lindner, C. Chojetzki, S. Brückner, M. Becker, M. Rothhardt, and H. Bartelt, "Thermal Regenerated Fiber Bragg Gratings in NonHydrogen Loaded Photosensitive Fibers," *Optics InfoBase Conference Papers*, vol. 17, no. 15, pp. 12523–12531, 2010, doi: 10.1364/bgpp.2010.btub3.

[34] E. Lindner *et al.*, "Arrays of regenerated fiber bragg gratings in non-hydrogen-loaded photosensitive fibers for high-temperature sensor networks," *Sensors*, vol. 9, no. 10, pp. 8377–8381, 2009, doi: 10.3390/s91008377.

[35] S. S. Chong, W. Y. Chong, S. W. Harun, and H. Ahmad, "Regenerated fibre Bragg grating fabricated on high germanium concentration photosensitive fibre for sensing at high temperature," *Opt Laser Technol*, vol. 44, no. 4, pp. 821–824, 2012, doi: 10.1016/j.optlastec.2011.11.024.

[36] K. Cook, L.-Y. Shao, and J. Canning, "Regeneration and helium: regenerating Bragg gratings in helium-loaded germanosilicate optical fibre," *Opt Mater Express*, vol. 2, no. 12, p. 1733, 2012, doi: 10.1364/ome.2.001733.

[37] B. Poumellec, "Links between writing and erasure (or stability) of Bragg gratings in disordered media," *J Alloys Compd*, vol. 239, no. 1, pp. 108–115, 1998, doi: 10.1016/s0022-3093(98)00726-1.

[38] C. Wang *et al.*, "A general method to synthesize and sinter bulk ceramics in seconds," *Science (1979)*, vol. 368, no. 6490, pp. 521–526, 2020, doi: 10.1126/science.aaz7681.

[39] F. Mumtaz *et al.*, "Highly-cascaded first-order sapphire optical fiber Bragg gratings fabricated by femtosecond Laser," *Opt Lett*, vol. 48,

no. 16, 2023, [Online]. Available: https://doi.org/10.1364/OL.495138
[40] D. R. Alla *et al.*, "Cascaded Sapphire Fiber Bragg Gratings Inscribed by Femtosecond Laser for Molten Steel Studies," *IEEE Trans Instrum Meas*, vol. PP, p. 1, 2023, doi: 10.1109/TIM.2023.3335530.
[41] D. Samiappan *et al.*, "Enhancing Sensitivity of Fiber Bragg Grating-Based Temperature Sensors through Teflon Coating," *Wirel Pers Commun*, vol. 110, no. 2, pp. 593–604, 2020, doi: 10.1007/s11277-019-06744-w.
[42] C. V. N. Bhaskar, S. Pal, and P. K. Pattnaik, "Recent advancements in fiber Bragg gratings based temperature and strain measurement," *Results in Optics*, vol. 5, 2021, doi: 10.1016/j.rio.2021.100130.
[43] W. Zhao and R. O. Claus, "Optical fiber grating sensors in multimode fibers," *Smart Mater Struct*, vol. 9, no. 2, pp. 212–214, 2000, doi: 10.1088/0964-1726/9/2/312.
[44] B. Liu *et al.*, "Design and Implementation of Distributed Ultra-High Temperature Sensing System with a Single Crystal Fiber," *Journal of Lightwave Technology*, vol. 36, no. 23, pp. 5511–5520, 2018, doi: 10.1109/JLT.2018.2874395.
[45] L. Hua, Y. Song, J. Huang, X. Lan, Y. Li, and H. Xiao, "Microwave interrogated large core fused silica fiber Michelson interferometer for strain sensing," *Appl Opt*, vol. 54, no. 24, p. 7181, 2015, doi: 10.1364/ao.54.007181.
[46] M. Roman *et al.*, "Temperature Monitoring in the Refractory Lining of a Continuous Casting Tundish Using Distributed Optical Fiber Sensors," *IEEE Trans Instrum Meas*, vol. 72, pp. 1–11, 2023, doi: 10.1109/TIM.2022.3225033.

Farhan Mumtaz (Member, IEEE) received the bachelor's degree in science from Punjab University Lahore, Lahore, Pakistan, in 2006, the master's degree in electronics from Quaid-i-Azam University Islamabad, Islamabad, Pakistan, in 2018, and the Ph.D. degree in information and communication engineering from the Wuhan University of Technology, Wuhan, China, in 2021.

In February 2022, he starts working with the Faculty of Electrical and Computer Engineering, Missouri University of Science and Technology, Rolla, MO, USA, where he is currently as an Assistant Research Professor. From 2007 to 2015, he worked for Huawei Technologies (Pvt.) Ltd., Islamabad, Pakistan, holding a number of important positions, including a Plan Control Manager, a Project Manager, and a Service Solution Manager. He has authored and coauthored more than 40 peer-reviewed high-ranking journal articles and has filed 01 US-patent application. His current research interests include sapphire crystalline fibers, fiber Bragg gratings, femtosecond micromachining of optoelectronic materials, Rayleigh and Brillion sensors, surface plasmons, biosensors, photonic crystal fiber design, and instrumentation of fiber optic sensors for energy and harsh environments in U.S. steelmaking industry.

Bohong Zhang (Member, IEEE) received a Ph.D. degree in electrical engineering from the Missouri University of Science and Technology, Rolla, MO, USA, in 2022. He is currently an Assistant Research Professor with the Lightwave Technology Laboratory, Department of Electrical and Computer Engineering, Missouri University of Science and Technology, Rolla, MO, USA. Dr. Zhang is a member of IEEE, SPIE, OSA, and the Association for Iron and Steel Technology (AIST) organization. His current research interests center around the advancement of optical and microwave sensors and instrumentation, focusing on their applications in intelligent infrastructures, biomedical sensing, and challenging environments.

Jeffrey D. Smith is currently a Professor of ceramic engineering with the Department of Materials Science and Engineering, Missouri University of Science and Technology, Rolla, MO, USA. His current research interests include high-temperature inorganic chemistry, materials characterization, high-temperature materials, and interactions between ceramics and molten materials.

Ronald J. O'Malley is currently the F. Kenneth Iverson Chair Professor of Steelmaking Technologies with the Department of Metallurgical Engineering, Missouri University of Science and Technology, Rolla, MO, USA. He is also the Director of the Kent D. Peaslee Steel Manufacturing Research Center (PSMRC), which is an industry-supported consortium with 18 industry members that support >U.S. $850k in research annually. He is also the PI for >U.S. $18M in research with the Department of Energy (DOE) in areas of sensor development, hydrogen steelmaking, and electric furnace optimization and is a Lecturer for several short courses in steel manufacturing, including the Brimacombe short course on continuous casting. He has more than 30 years of experience in the metals manufacturing industry at Alcoa, Alcoa Center, New Kensington, PA, USA, Armco/AK Steel, Middletown, OH, USA, and Nucor Steel, LLC, Decatur, AL, USA. He has authored more than 150 journal and conference proceedings papers, over 70 invited and contributed presentations, and holds three U.S. patents. His current research interests include H2 Ironmaking, EAF steelmaking, steel refining, clean steel processing and inclusion engineering, steel-refractory interactions, continuous casting, deformation processing, sensor development for harsh steelmaking environments, and new steel grade development.

Dr. O'Malley is an AIST Distinguished Member and a fellow. He was the President of the Association for Iron and Steel Technology (AIST) from 2019 to 2021. He is currently serving on the board of trustees and is president elect designate of AIME.

Rex E. Gerald II received the B.A. degree (Hons.) in chemistry from The University of Chicago (UC), Chicago, IL, USA, in 1984, and a conjoint Ph.D. degree in physical chemistry from the University of Illinois Chicago (UIC), Chicago, and the Max Planck Institute (MPI), Heidelberg, Germany, in 1994. He is currently a Research Professor with the Lightwave Technology Laboratory, Department of Electrical and Computer Engineering, Missouri University of Science and Technology (MS&T), Rolla, Mo, USA. He holds 27 U.S. patents and coauthored more than 100 publications from research investigations conducted at UC, UIC, MPI, Argonne National Laboratory, and MS&T.

Jie Huang (Senior Member, IEEE) received a Ph.D. in electrical engineering from Clemson University, Clemson, SC, USA, in 2015. He is currently the Roy A. Wilkens Endowed Associate Professor in the Department of Electrical and Computer Engineering at Missouri University of Science and Technology, Rolla, MO, USA. He has established the Lightwave Technology Laboratory (LTL), Rolla, with a strong track record of sustained research funding, high-quality journal publications, and state-of-the-art research infrastructures with cutting-edge capabilities. He has authored or co-authored over 150 refereed articles, 80 conference papers, one book chapter, and ten U.S. patents, all in the arena of advanced sensors. His current research interests include the development of optical and microwave sensors and instrumentation for applications in energy, intelligent infrastructures, clean environments, biomedical sensing, and harsh environments.